MATCH
Communications in Mathematical and in Computer Chemistry

MATCH Commun. Math. Comput. Chem. **93** (2025) 99–128
ISSN: 0340–6253
doi: 10.46793/match.93-1.099M

A Mathematical Approach to Ullmann Reaction: ANFIS Computing of a Chemical Retrial Queue Model under Hybrid Vacation

N. Micheal Mathavavisakan[a], K. Indhira[a,*]

[a] *Department of Mathematics, School of Advanced Sciences, Vellore Institute of Technology, Vellore - 632 014, Tamil Nadu, India*
michealmathava.visakan2020@vitstudent.ac.in, kindhira@vit.ac.in

(Received February 20, 2024)

Abstract

Herein, we developed the first report on the chemical retrial queue and hybrid vacation process for the significant Ullmann coupling for enhanced high-throughput reaction discovery. The problem of controlling the waiting time for chemical retrials is addressed here. We incorporated the supplementary variables method (SVT) and generated the steady-state probability generating function (PGF) for system size and orbit size. Important cases are outlined, and a few key metrics are utilized to evaluate system performance. Additionally, the impact of changing certain system parameters has also been analyzed via numerical examples. One particularly interesting aspect of this research is the comparison of neuro-fuzzy technique results with validation results utilizing the "adaptive neuro-fuzzy inference system" (ANFIS).

1 Background and preliminaries

Chemical processes like "chemical queueing models" lie at the heart of queuing models, and they are considered the "holy grail" of queuing models. In the realm of queueing models, chemical queueing models is bur-

*Corresponding author(K. Indhira).

geoning owing to its great deal of attention among mathematicians and chemists. In these models, a molecule is modeled as an endlessly long chain of atoms united by links of equal length. The linkages are sensitive to random shocks, which cause the atoms to move and the molecule to spread, as discussed by Bohm and Homik [1]. In the context of chemical physics, Stochmayer et al. [2] were the first to explore the chemical queueing model phenomenon. Following the efforts from Stochmayer, Conolly et al. [3] analyzed chemical queueing processes using the direct approach. With the help of a uniformization technique, Tarabia and El-Baz [4,5] have provided a comprehensive analysis. They posed the system of partial difference equations whose solutions are the transition functions of the embedded discrete-time Markov chain and further made some educated guesses as to what those solutions may be, and finally proved it by induction. Stanislav Tsitkov [6] found a way to use a queueing model to investigate the results of random factors on a N-step reaction cascade catalysed by N enzymes immobilized on a scaffold. Of late, Alshreef and Tarabia [7] looked into the transient analysis of the chemical queue with disasters and server maintenance.

Queuing systems are mathematically abbreviated frameworks that characterize congestion. In general, a queueing system emerged whenever 'customers' demand 'service' from a resource. Queuing theory has numerous business implications in real life. Queuing theory can address staffing, planning, and customer service deficiencies, and is widely used as a tool for operations management. The objective of queueing theory is to devise balanced networks that serve consumers promptly and effectively while remaining economically viable. Customers who are blocked often leave the service facility for a short period of time before returning at a later date. This happens in many real-world and technological contexts. Before making another attempt to occupy a server, a customer who has been temporarily banned will wait in a virtual waiting area known as orbit. Retrial queues are used to represent these kinds of occurrences. In many implementations, the retrial rate is proportional to the number of consumers in the orbit because they often behave independently of one another. Falin and Templeton [10], Artalejo et al. [11], among others, have conducted

extensive studies on the RQ.

A server must briefly suspend all service and be unreachable to its principal consumers in order to establish a vacation queueing mechanism. This time away from work is referred to as a vacation. During working vacation periods (WV), nevertheless, the server delivers service to clients at a reduced rate. The providing of network service, internet service, file transfer service, and postal service are among its numerous applications. A single server retrial queueing system (SSRQ) was introduced by Arivudainambi et al. [12] with WV. Recent time Chandrasekaran et al. [13] developed a concise review on WV queueing techniques. New RQ models with brakes and WV were addressed by Rajadurai [14]. Revathi [15] looked into several different types of retrial queuing systems, including ones with consumer search, optional re-service and delayed repairs.

For various reasons, consumers in a queue may need to be serviced on multiple occasions. Customer service that isn't satisfactory can be tried again and again until it is. Several real-world scenarios lend themselves to stochastic modeling, which includes these queueing models. Such instances of queuing are known as feedback. In data transmission, for instance, a packet sent from the source to the destination may be returned and the process may resume until the packet is successfully sent. Maragathasundari and Balamurugan [16] conducted a research on the $M^{[X]}/G/1$ feedback queue, which included two phases of repair times as well as general delay duration. Gnanasekar and Kandaiyan [17] looked at the $M/G/1$ RQ with feedback and delayed repair in accordance with the WV policy with impatient customers.

The molecular mechanism behind the Ullmann reaction

The topic of long-standing interest in synthetic chemistry is building value-added products from chemical feedstocks, and it is an attractive topic and of paramount importance to drug development. Among them, sustainable synthesis is an up-and-coming methodology that entices chemists to bypass the use of stoichiometric reagents and employ cost-effective first-row transition metal catalysts. Along the line, copper is in the upper hand owing to earth-abundant and its versatile stable oxidation states [Cu(0), Cu(I)

and Cu(II)]. Inspired by what has been mentioned above, it is of great desire to employ copper catalysis in the synthesis of symmetric biaryls by means of "classic" Ullmann coupling. A typical Ullmann coupling [8] involves combining the aryl halide with an excessive amount of copper at elevated temperatures (210 – 260 °C) to produce biaryls. A schematic representation of the Ullmann reaction and its mechanism is given in Fig. 1. The reaction proceeds via the oxidative addition of iodobenzene to copper to yield organocuprate and further oxidative addition of another iodobenzene which results in copper intermediate with Cu(III). Then reductive elimination occurs to yield the desired biaryl product [9].

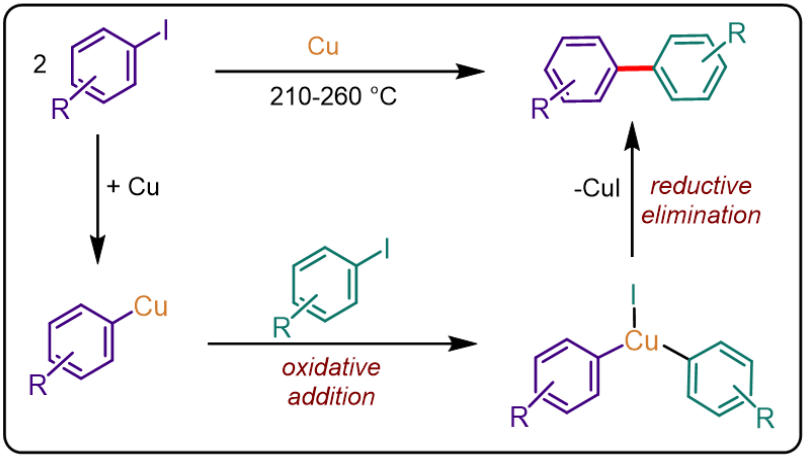

Figure 1. Mechanism of Ullmann Reaction

In the Ullmann reaction, the iodobenzene (arrival) undergoes number of reactions with copper (server) to form biphenyl (output). Since the copper reacts with a single iodobenzene at a time, the remaining iodobenzenes will be waiting in orbit to get reacted or else will remain unreacted in the reaction vessel. After the initial reaction gets over the iodobenzenes which is waiting in the orbit will undergo the reaction one by one and then forms biphenyl. When orbit becomes empty, the server switch on working vacation and the service becomes slower. If any iodobenzene is present during the working vacation period, it will get reacted slowly and

then form biphenyl. If there is no iodobenzene then the vessel will undergo complete vacation. After the completion of CV, if there is no iodobenzene in the system, the server remains in CV, whereas if any iodobenzene enters the system the CV will switch to normal busy mode and start to provide service.

In this paper, in order to accomodate the Ullmann's reaction, we generalized the chemical queue by introducing the concept of hybrid vacation. Here, we have visualised the chemical retrial queue for the first time in which no one else has done before. To perform organic synthesis and drug discovery, the Ullmann coupling reaction has emerged as an effective and incredibly useful tool. Copper-catalyzed Ullmann reactions have recently been greatly advanced through the use of novel ligands and intermediary synthetic tools. Green synthetic methodologies, including metal, ligand and additive-free conditions, recyclable heterogeneous catalysts, and microwave-assisted synthesis, are expected to continue to have a significant impact on this field, which is undergoing a number of exciting and rapid developments due to the Ullmann coupling reactions.

This research is being done with the intention of determining the queue size and orbit size distributions, both of which will be utilized in the process of determining the system's other behaviour metrics. As for the outline of our piece, here it is: we provide a comprehensive explanation of the queueing paradigm in section 2. The steady-state (SS) behaviour of the system and the random epoch probability generating function (PGF) of the queue size are described in detail in section 3. Section 4 contains a number of crucial indicators of the system's behaviour. Findings are presented both numerically and visually in section 5. In section 6, the findings from the neuro-fuzzy analysis of the system as well as the outcomes of changing the system's parameters are visually examined and explained. The paper finishes with a summary of its key themes in section 7.

2 The model's overview and applicability in real life

Under hybrid vacation (HV) policy, we provide a $M/G/1$ chemical RQ model. The precise justification of our model is as follows:

The arrival process: According to the Poisson process, iodobenzene will undergo reaction at the rate γ.

The retrial process: A new iodobenzene will immediately be subjected to reaction when it arrives and discovers that the copper (server) is available (after taking a complete vacation). In the alternative, if arriving iodobenzene discover that the server is busy or providing lower speed service, the arrivals either leave the service area with a probability of $\bar{\xi} = (1 - \xi)$ or join the blocked area called an orbit with a probability of ξ in accordance with FCFS discipline. This means that only the iodobenzene which is currently at the front of the orbit queue will get reacted. After a certain amount of time, iodobenzene will try again to react. Inter retrial period have a general distribution $\mathcal{G}(x)$ with corresponding "Laplace-Stieltjes Transform" (LST) $\mathcal{G}^*(\varphi)$.

Regular service process: When a new iodobenzene arrives and discovers that the copper is available, then the copper will immediately starts reacting, and subsequent iodobenzenes will join the orbit. The regular service period represents a general distribution and it is defined by the arbitrary variable $\mathcal{H}_b$ with distribution function $\mathcal{H}_b(\varpi)$ having LST $\mathcal{H}_b^*(\varphi)$.

Hybrid vacation policy: The vacation process is a hybrid process in which the copper can still provide service but at a slower rate when the orbit becomes idle and the vacation period takes an exponential distribution with parameter ω. If there are iodobenzene available during the WV period, the copper will remain in WV and renders service to the available iodobenzene. However, if the system becomes empty during WV, the server will go into CV, and it follows an exponential distribution with parameter η. After the completion of CV, if there is no iodobenzene in the system, the server remains in CV with probability $\overline{q}(= 1 - q)$, whereas if iodobenzene enters the system, the CV will switch to normal busy mode and start providing service to the new iodobenzene with probability q.

During the HV period, the service period is assessed by a random variable $\mathcal{H}_v$ with distribution function $\mathcal{H}_v(\varpi)$ and LST $\mathcal{H}_v^*(\varphi)$.

The stochastic processes of the system are seen as being completely independent of one another. The diagrammatic illustration of the model that can be found in Fig. 2.

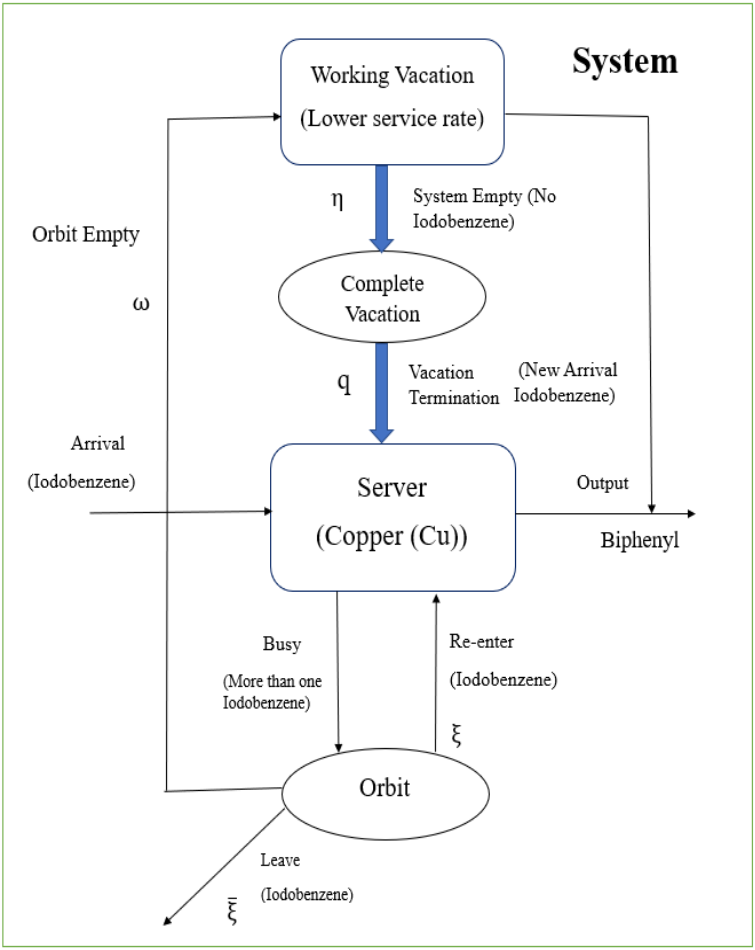

Figure 2. Pictorial representation of the model

2.1 Implementation of the model in real Life

Our approach may have some useful applications in the production process. Assume that a manufacturing plant contains a machine that is shared by all of the units that make up the plant (these units are termed customers). Two people, one skilled worker and his trainee, are needed to run the machine. The machine is only operated by the apprentice to provide service to the units when the skilled worker is away on vacation (this type of absence is known as "working vacation"), and the apprentice's rate of service is typically slower than that of the skilled worker. In the event that the device is currently servicing a large number of customers, a new arrival unit will be directed to join a waiting line, which is analogous to the retry queue. In any other case, the unit will be served right away. If an additional external unit arrives before the skilled worker can make contact with the next unit on the list, then the skilled worker will not complete the service and move on to the next unit on the list. The contact time is presumed to be distributed evenly across the population (which is called general retrial time). When the skilled worker arrives at the front of the line and discovers that there are no units available, he will be required to take a break from his labour in the form of a vacation. During the time that the skilled worker is away on vacation, his apprentice will provide service to the units at a slightly reduced speed. In the event that there is no unit in the system, both the skilled worker and the apprentice will go into a period of complete vacation. No matter the apprentice has served the unit, the skilled worker will restart his service if there is any unit that arrives at that time in order to guarantee the quality of the skilled worker's service. This is done to reduce the skilled worker idle time.

Other domains where this paradigm has been put to use include stochastic production and inventory systems with a multipurpose production facility, packet switched networks, and the transport of emails between servers using the Simple Mail Transfer Protocol (SMTP).

3 System's steady state analysis

This section begins by formulating the steady-state equations (SS) for the RQ system. These equations take into account the elapsed retrial period, the elapsed service time, and the elapsed lower-speed service times as supplementary variables (SV). Calculations are made to determine the PGF of the total number of iodobenzene in the orbit and system, in addition to the orbit length generating functions for a number of different server states.

3.1 Probabilities and notations for the steady state

It is assumed in SS that $\mathcal{G}(0) = 0$, $\mathcal{G}(\infty) = 1$, $\mathcal{H}_b(0) = 0$, $\mathcal{H}_b(\infty) = 1$ and $\mathcal{H}_v(0) = 0$, $\mathcal{H}_v(\infty) = 1$ are cont., at $\varpi = 0$. So that the func. $g(\varpi)$, $\zeta_b(\varpi)$, $\zeta_v(\varpi)$, are the hazard rates for retrial, service and slower pace service respectively.

$$g(\varpi)d\varpi = \frac{d\mathcal{G}(\varpi)}{1 - \mathcal{G}(\varpi)}$$
$$\zeta_b(\varpi)d\varpi = \frac{d\mathcal{H}_b(\varpi)}{1 - \mathcal{H}_b(\varpi)}$$
$$\zeta_v(\varpi)d\varpi = \frac{d\mathcal{H}_v(\varpi)}{1 - \mathcal{H}_v(\varpi)}$$

Apart from it, let $\mathcal{G}^0(\breve{\varrho})$,$\mathcal{H}_b^0(\breve{\varrho})$ and $\mathcal{H}_v^0(\breve{\varrho})$ be the elapsed time for retrial, normal service and slower-rate service at time $\breve{\varrho}$ respectively.

3.2 The proposed model's steady state equations

Let's define the random variable for the construction of this retrial QS

$$\Psi(\breve{\varrho}) = \begin{cases} 0, & \text{if the server is available and in hybrid vacation time} \\ 1, & \text{if the server is available and in normal service time} \\ 2, & \text{if the server is unavailable and in normal service at time } \breve{\varrho} \\ 3, & \text{if the server is unavailable and in hybrid vacation at time } \breve{\varrho} \end{cases}$$

In this section, we concentrate on the use of the bivariate Markov

process to characterize the system's state at time $\{\Psi(\breve{\varrho}),\ \mathcal{Y}(\breve{\varrho});\ \breve{\varrho} \geq 0\}$, here $\Psi(\breve{\varrho})$ represent the server state $(0, 1, 2, 3)$ depending on whether the server is free or busy on both normal service and WV periods. $\mathcal{Y}(\breve{\varrho})$ denotes the number of iodobenzene in the orbit. If $\Psi(\breve{\varrho}) = 1$ and $\mathcal{Y}(\breve{\varrho}) > 0$, then $\mathcal{G}^0(\breve{\varrho})$ is equivalent to the elapsed retrial time. If $\Theta(\breve{\varrho}) = 2$ and $\mathcal{Y}(\breve{\varrho}) \geq 0$, then $\mathcal{H}_b^0(\breve{\varrho})$ is equivalent to the elapsed time of the iodobenzene served in normal busy period. If $\Psi(\breve{\varrho}) = 3$ and $\mathcal{Y}(\breve{\varrho}) \geq 0$, then $\mathcal{H}_v^0(\breve{\varrho})$ is equivalent to the elapsed time of the iodobenzene being served in lower rate service period.

3.3 Model's ergodicity condition

Theorem 1. *The embedded Markov chain (MC)* $\{\mathcal{F}_m; m\epsilon\mathcal{M}\}$ *is considered ergodic iff the system is stable at* $\Lambda < \mathcal{G}^*(\gamma)$*, where* $\Lambda = \gamma\xi\mathcal{E}(\mathcal{H}_b)$.

Proof. The requirement of ergodicity can be easily confirmed by using Foster's criteria [18], which state that the chain $\{\mathcal{F}_m; m \in \mathcal{M}\}$ is an irreducible and aperiodic chain. These criteria assert that the chain can not be reduced and that it has a periodic structure. Assuming that $e(r)$, is non-negative, $r \in \mathcal{M}$, and $\delta > 0$, the MC is ergodic, and the mean value $\nu_r = \mathcal{E}[e(u_{m+1}) - e(u_m)/v_m = r]$ with certain restricted exemptions r's, $r \in \mathcal{M}$ and $\nu_r \leq -\delta\ \forall\ r \in \mathcal{M}$,. In this particular instance, we will be concentrating on the function written as $e(r) = r$. After that, we get:

$$\nu_r = \begin{cases} \gamma\xi\mathcal{E}(\mathcal{H}_b) - \mathcal{G}^*(\gamma), & \text{if } r\text{=1,2,...} \\ \gamma\xi\mathcal{E}(\mathcal{H}_b) - 1, & \text{if } r\text{=0} \end{cases}$$

In this particular instance, $\gamma\xi\mathcal{E}(\mathcal{H}_b) < \mathcal{G}^*(\gamma)$ is undeniably a requirement for ergodicity.

According to the statements made by Humblett et al. [19], the necessary condition will be satisfied if the MC $\{\mathcal{F}_m; m\epsilon\mathcal{M}\}$ meets Kaplan's status. More specifically, this means that $\nu_r < \infty\ \forall\ r \geq 0$ and $\exists\ r_0 \in \mathcal{M}$ such that $\nu_r \geq 0$ for $r \geq r_0$, then the necessary requirement has been fulfilled. $\mathcal{V} = (v_{qr})$ is the the unit-step transition matrix of $\{\mathcal{F}_m; m \in \mathcal{M}\}$ for $r < q - j$ and $q > 0$. The non-ergodic nature of the Markov chain can be

inferred if $\Lambda \geq \mathcal{G}^*(\gamma)$ is satisfied. ■

Let $\{\breve{\varrho}_n; n = 1, 2, ...\}$ be the series of epochs where a service period ends or begins. A sequence of random vectors that can be represented by the equation $\mathcal{F}_n = \{\Psi(\breve{\varrho}_n+), \mathcal{Y}(\breve{\varrho}_n+)\}$. The Markov chain that was produced by embedding RQ's into the system. As a consequence of Theorem (3.1) $\{\mathcal{F}_n; n \in N\}$ is ergodic iff $\Lambda < \mathcal{G}^*(\gamma)$, in necessary for our structure to maintain its stability, where $\Lambda = \gamma\xi\mathcal{E}(\mathcal{H}_b)$.

For the procedure $\{\mathcal{Y}(\breve{\varrho}), \breve{\varrho} \geq 0\}$, we describe the probabilities $\Pi_0(\breve{\varrho}) = \mathcal{P}\{\Psi(\breve{\varrho}) = 0, \mathcal{Y}(\breve{\varrho}) = 0\}$, $\Upsilon_0(\breve{\varrho}) = \mathcal{P}\{\Psi(\breve{\varrho}) = 1, \mathcal{Y}(\breve{\varrho}) = 0\}$. $\Pi_0(\breve{\varrho})$ is the probability that the system is free at time $(\breve{\varrho})$ and the copper is in working vacation. $\Upsilon_0(\breve{\varrho})$ is the probability that the system is free at time $(\breve{\varrho})$ and the copper is in regular busy period and the probability dens. are

$\Upsilon_n(\varpi, \breve{\varrho})d\varpi = \mathcal{P}\{\Psi(\breve{\varrho}) = 1, \mathcal{Y}(\breve{\varrho}) = n, \varpi \leq \mathcal{G}^0(\breve{\varrho}) < \varpi + d\varpi\}$,
for $\breve{\varrho} \geq 0$, $\varpi \geq 0$ and $n \geq 1$.
$\Theta_{b,n}(\varpi, \breve{\varrho})d\varpi = \mathcal{P}\{\Psi(\breve{\varrho}) = 2, \mathcal{Y}(\breve{\varrho}) = n, \varpi \leq \mathcal{H}_b^0(\breve{\varrho}) < \varpi + d\varpi\}$,
for $\breve{\varrho} \geq 0$, $\varpi \geq 0$ and $n \geq 0$.
$\Delta_{v,n}(\varpi, \breve{\varrho})d\varpi = \mathcal{P}\{\Psi(\breve{\varrho}) = 3, \mathcal{Y}(\breve{\varrho}) = n, \varpi \leq \mathcal{H}_v^0(\breve{\varrho}) < \varpi + d\varpi\}$,
for $\breve{\varrho} \geq 0$, $\varpi \geq 0$ and $n \geq 0$.

For now, let's assume the stability criterion is met and do some assigning based on that $\Pi_0 = lim_{\breve{\varrho}\to\infty}\Pi_0(\breve{\varrho})$, $\Upsilon_0 = lim_{\breve{\varrho}\to\infty}\Upsilon_0(\breve{\varrho})$ and limiting densities are
$\Upsilon_n(\varpi) = lim_{\breve{\varrho}\to\infty}\Upsilon_n(\varpi, \breve{\varrho})$; $\Theta_{b,n}(\varpi) = lim_{\breve{\varrho}\to\infty}\Theta_{b,n}(\varpi, \breve{\varrho})$;
$\Delta_{v,n}(\varpi) = lim_{\breve{\varrho}\to\infty}\Delta_{v,n}(\varpi, \breve{\varrho})$.

The following set of equations was constructed using the supplementary variable technique.

$$\gamma\Upsilon_0 = (\omega + \eta)q\Pi_0 \tag{1}$$

$$(\gamma + \omega + \eta)\Pi_0 = (\omega + \eta)\overline{q}\Pi_0 + \int_0^\infty \Theta_{b,0}(\varpi)\zeta_b(\varpi)d\varpi + \int_0^\infty \Delta_{v,0}(\varpi)\zeta_v(\varpi)d\varpi \tag{2}$$

$$\frac{d}{d\varpi}\Upsilon_n(\varpi) + (\gamma + g(\varpi))\Upsilon_n(\varpi) = 0, n \geq 1 \tag{3}$$

$$\frac{d}{d\varpi}\Theta_{b,0}(\varpi) + (\gamma + \zeta_b(\varpi))\Theta_{b,0}(\varpi) = \gamma\bar{\xi}\Theta_{b,0}(\varpi), n = 0 \tag{4}$$

$$\frac{d}{d\varpi}\Theta_{b,n}(\varpi) + (\gamma + \zeta_b(\varpi))\Theta_{b,n}(\varpi) = \gamma\xi\Theta_{b,n-1}(\varpi) + \gamma\bar{\xi}\Theta_{b,n-1}(\varpi), n \geq 1 \tag{5}$$

$$\frac{d}{d\varpi}\Delta_{v,0}(\varpi) + (\gamma + \omega + \eta + \zeta_v(\varpi))\Delta_{v,0}(\varpi) = \gamma\bar{\xi}\Delta_{v,0}(\varpi), n = 0 \tag{6}$$

$$\frac{d}{d\varpi}\Delta_{v,n}(\varpi) + (\gamma + \omega + \eta + \zeta_v(\varpi))\Delta_{v,n}(\varpi) = \gamma\xi\Delta_{v,n-1}(\varpi) + \gamma\bar{\xi}\Delta_{v,n-1}(\varpi), n \geq 0 \tag{7}$$

Here are the criterion for the SS boundary for $\varpi = 0$:

$$\Upsilon_n(0) = \int_0^\infty \Theta_{b,n}(\varpi)\zeta_b(\varpi)d\varpi + \int_0^\infty \Delta_{v,n}(\varpi)\zeta_v(\varpi)d\varpi, n \geq 1 \tag{8}$$

$$\Theta_{b,n}(0) = \int_0^\infty \Upsilon_{n+1}(\varpi)g(\varpi)d\varpi + \gamma\int_0^\infty \Upsilon_n(\varpi)d\varpi + (\omega + \eta)\int_0^\infty \Delta_{v,n}(\varpi)d\varpi, n \geq 1 \tag{9}$$

$$\Theta_{b,0}(0) = \int_0^\infty \Upsilon_1(\varpi)g(\varpi)d\varpi + (\omega + \eta)\int_0^\infty \Delta_{v,0}(\varpi)d\varpi + \gamma\Upsilon_0, n = 0 \tag{10}$$

$$\Delta_{v,n}(0) = \begin{cases} \gamma\Pi_0, & n = 0 \\ 0, & n \geq 1 \end{cases} \tag{11}$$

The criteria for normalization is given by,

$$\Pi_0 + \Upsilon_0 + \sum_{n=1}^{\infty}\int_0^\infty \Upsilon_n(\varpi)d\varpi + \sum_{n=0}^{\infty}\left(\int_0^\infty \Theta_{b,n}(\varpi)d\varpi + \int_0^\infty \Delta_{v,n}(\varpi)d\varpi\right) = 1 \tag{12}$$

3.4 The steady state solution

Specifically, the GFs for $\mid \vartheta \mid < 1$ that are needed to solve the aforementioned equations have the form.

$$\Upsilon(\varpi,\vartheta)=\sum_{n=1}^{\infty}\Upsilon_n(\varpi)\vartheta^n;\Upsilon(0,\vartheta)=\sum_{n=1}^{\infty}\Upsilon_n(0)\vartheta^n;$$

$$\Theta_b(\varpi,\vartheta)=\sum_{n=0}^{\infty}\Theta_{b,n}(\varpi)\vartheta^n;\Theta_b(0,\vartheta)=\sum_{n=0}^{\infty}\Theta_{b,n}(0)\vartheta^n;$$

$$\Delta_v(\varpi,\vartheta)=\sum_{n=0}^{\infty}\Delta_{v,n}(\varpi)\vartheta^n;\Delta_v(0,\vartheta)=\sum_{n=0}^{\infty}\Delta_{v,n}(0)\vartheta^n.$$

Now multiply the SS equation and SS boundary conditions from (3) to (11) by ϑ^n and summing over n, $(n=0,1,2,...)$

$$\frac{\partial}{\partial\varpi}\Upsilon(\varpi,\vartheta)+(\gamma+g(\varpi))\Upsilon(\varpi,\vartheta)=0 \tag{13}$$

$$\frac{\partial}{\partial\varpi}\Theta_b(\varpi,\vartheta)+(\gamma\xi(1-\vartheta))+\zeta_b(\varpi))\Theta_b(\varpi,\vartheta)=0 \tag{14}$$

$$\frac{\partial}{\partial\varpi}\Delta_v(\varpi,\vartheta)+(\gamma\xi(1-\vartheta)+\omega+\eta+\zeta_v(\varpi))\Delta_v(\varpi,\vartheta)=0 \tag{15}$$

$$\begin{aligned}\Upsilon(0,\vartheta)=&\int_0^{\infty}\Theta_b(\varpi,\vartheta)\zeta_b(\varpi)d\varpi+\int_0^{\infty}\Delta_v(\varpi,\vartheta)\zeta_v(\varpi)d\varpi\\&-[(\gamma+\omega+\eta)\Pi_0-(\omega+\eta)\bar{q}\Upsilon_0]\end{aligned} \tag{16}$$

$$\begin{aligned}\Theta_b(0,\vartheta)=&\frac{1}{\vartheta}\int_0^{\infty}\Upsilon(\varpi,\vartheta)g(\varpi)d\varpi+\gamma\int_0^{\infty}\Upsilon(\varpi,\vartheta)d\varpi\\&+(\omega+\eta)\int_0^{\infty}\Delta_v(\varpi,\vartheta)d\varpi\end{aligned} \tag{17}$$

$$\Delta_v(0,\vartheta)=\gamma\Pi_0 \tag{18}$$

By completing the solutions to the partial differential equations (13)

and (15), we have

$$\Upsilon(\varpi,\vartheta)=\Upsilon(0,\vartheta)[1-\mathcal{G}(\varpi)]e^{-\gamma\varpi} \tag{19}$$

$$\Theta_b(\varpi,\vartheta)=\Theta_b(0,\vartheta)[1-\mathcal{H}_b(\varpi)]e^{-\mathcal{H}_1(\vartheta)\varpi} \tag{20}$$

$$\Delta_v(\varpi,\vartheta)=\Delta_v(0,\vartheta)[1-\mathcal{H}_v(\varpi)]e^{-\mathcal{H}_2(\vartheta)\varpi} \tag{21}$$

where $\mathcal{H}_1(\vartheta)=\gamma\xi(1-\vartheta)$, and $\mathcal{H}_2(\vartheta)=\omega+\eta+\gamma\xi(1-\vartheta)$

After some mathematical calculations, we obtain

$$\Theta_b(0,\vartheta)=\frac{\Upsilon(0,\vartheta)}{\vartheta}\{\mathcal{G}^*(\gamma)+\vartheta[1-\mathcal{G}^*(\gamma)]\}+\gamma\Pi_0\mathcal{H}(\vartheta) \tag{22}$$

where $\mathcal{H}(\vartheta)=\frac{\omega+\eta}{\omega+\eta+\gamma\xi(1-\vartheta)}\ (1-\mathcal{H}_v^*(\mathcal{H}_2(\vartheta)))$

$$\Upsilon(0,\vartheta)=\Theta_b(0,\vartheta)\mathcal{H}_b^*(\mathcal{H}_1(\vartheta))+\Delta_v(0,\vartheta)\mathcal{H}_v^*(\mathcal{H}_2(\vartheta))-[\gamma+(\omega+\eta)q]\Pi_0 \tag{23}$$

Further, we get a combination of (11) and (22) in (23),

$$\begin{aligned}\Upsilon(0,\vartheta)\{\vartheta-[\mathcal{G}^*(\gamma)+\vartheta(1-\mathcal{G}^*(\gamma))]\mathcal{H}_b^*(\mathcal{H}_1(\vartheta))\}\\ =\vartheta\Pi_0\{\gamma[\mathcal{H}(\vartheta)\mathcal{H}_b^*(\mathcal{H}_1(\vartheta))+\mathcal{H}_v^*(H_2(\vartheta))-1]-(\omega+\eta)q\}\end{aligned} \tag{24}$$

In the theory that follows, we are open to investigating the marginal orbit length distribution that are brought about by the system state of the server.

Theorem 2. *Under the stability requirement, $\Lambda<\mathcal{G}^*(\gamma)$ provides the stationary distribution of the number of iodobenzene in the orbit when the server is available, busy, reduced rate service, and the probability that the server is available given by,*

$$\Upsilon(\vartheta)=\frac{\mathcal{N}e(\vartheta)}{\mathcal{D}e(\vartheta)} \tag{25}$$

$$\mathcal{N}e(\vartheta) = \vartheta\Pi_0\{\gamma[\mathcal{H}(\vartheta)\mathcal{H}_b^*(\mathcal{H}_1(\vartheta)) + \mathcal{H}_v^*(H_2(\vartheta)) - 1] - (\omega+\eta)q\}$$

$$\mathcal{D}e(\vartheta) = \vartheta - \{\mathcal{G}^*(\gamma) + \vartheta[1-\mathcal{G}^*(\gamma)]\}\mathcal{H}_b^*(\mathcal{H}_1(\vartheta))$$

$$\Theta_b(\vartheta) = \frac{\gamma\Pi_0(1-\mathcal{H}_b^*(\mathcal{H}_1(\vartheta)))}{\mathcal{H}_1(\vartheta)\mathcal{D}e(\vartheta)}\{\vartheta\mathcal{H}(\vartheta) + [\mathcal{H}_v^*(\mathcal{H}_2(\vartheta)) - 1] [\mathcal{G}^*(\gamma) + \vartheta[1-\mathcal{G}^*(\gamma)]]\} \tag{26}$$

$$\Delta_v(\vartheta) = \frac{\gamma\Pi_0}{\omega+\eta}\mathcal{H}(\vartheta) \tag{27}$$

where,

$$\Pi_0 = \frac{\mathcal{G}^*(\gamma) + \gamma\xi\mathcal{E}(\mathcal{H}_b)}{\mathcal{G}^*(\gamma) + \gamma\xi\mathcal{E}(\mathcal{H}_b)\mathcal{H}_v^*(\omega+\eta) + \gamma[1-\mathcal{H}_v^*(\omega+\eta)] \left\{\frac{\mathcal{G}^*(\gamma)+\xi(1-\mathcal{G}^*(\gamma))}{\omega+\eta} - \mathcal{G}^*(\gamma)\mathcal{E}(\mathcal{H}_b)(1-\xi)\right\} + q\xi(\omega+\eta)[\mathcal{G}^*(\gamma)-1]} \tag{28}$$

$$\Upsilon_0 = \frac{\{(\omega+\eta)q[\mathcal{G}^*(\gamma) + \gamma\xi\mathcal{E}(\mathcal{H}_b)]\}\Pi_0}{\mathcal{G}^*(\gamma) + \gamma\xi\mathcal{E}(\mathcal{H}_b)\mathcal{H}_v^*(\omega+\eta) + \gamma[1-\mathcal{H}_v^*(\omega+\eta)] \left\{\frac{\mathcal{G}^*(\gamma)+\xi(1-\mathcal{G}^*(\gamma))}{\omega+\eta} - \mathcal{G}^*(\gamma)\mathcal{E}(\mathcal{H}_b)(1-\xi)\right\} + q\xi(\omega+\eta)[\mathcal{G}^*(\gamma)-1]} \tag{29}$$

Proof. Taking the eqns. (19)-(21) and integrate with respect to ϖ and calculate the probability generating function $\Upsilon(\vartheta) = \int_0^\infty \Upsilon(\varpi,\vartheta)d\varpi$, $\Theta_b(\vartheta) = \int_0^\infty \Theta_b(\varpi,\vartheta)d\varpi$, $\Delta_v(\vartheta) = \int_0^\infty \Delta_v(\varpi,\vartheta)d\varpi$. We calculate the probability that the server is empty using the normalization condition (Π_0) by establishing functions as, when there is no iodobenzene in the orbit $\vartheta = 1$ in (25)-(27) and whenever the condition of L'Hospital is needed, we get $\Pi_0 + \Upsilon_0 + \Upsilon(1) + \Theta_b(1) + \Delta_v(1) = 1$. ■

Theorem 3. *Utilizing the PGF function, the number of iodobenzene in the system and the orbit size distribution at a stationary point of period are calculated under the stability constraint* $\Lambda < \mathcal{G}^*(\gamma)$,

$$\mathcal{K}(\vartheta) = \frac{\mathcal{N}e(\vartheta)}{\mathcal{D}e(\vartheta)} \tag{30}$$

$$\begin{aligned}\mathcal{N}e(\vartheta) =&\Pi_0\Bigg\{De(\vartheta)\Bigg[\left(\frac{\gamma}{\omega+\eta}\right)[(\omega+\eta)+\gamma\vartheta\mathcal{H}(\vartheta)]+(\omega+\eta)q\Bigg]\\&+\vartheta\mathcal{H}_1(\vartheta)(1-\mathcal{G}^*(\gamma))\{[\mathcal{H}_b^*(\mathcal{H}_1(\vartheta))\mathcal{H}(\vartheta)+\mathcal{H}_v^*(\mathcal{H}_2(z))]-1\}\\&+\vartheta\gamma(1-\mathcal{H}_b^*(\mathcal{H}_1(\vartheta)))\{\vartheta\mathcal{H}(\vartheta)+[\mathcal{H}_v^*(\mathcal{H}_2(\vartheta))-1]\\&[\mathcal{G}^*(\gamma)+\vartheta[1-\mathcal{G}^*(\gamma)]]\}\Bigg\}\\\mathcal{D}e(\vartheta) =&\mathcal{H}_1(\vartheta)\{\vartheta-\{\mathcal{G}^*(\gamma)+\vartheta[1-\mathcal{G}^*(\gamma)]\}\mathcal{H}_b^*(\mathcal{H}_1(\vartheta))\}\end{aligned}$$

$$\mathcal{K}_0(\vartheta)=\frac{\mathcal{N}e_0(\vartheta)}{\mathcal{D}e(\vartheta)} \tag{31}$$

$$\begin{aligned}\mathcal{N}e_0(\vartheta) =&\Pi_0\Bigg\{De(\vartheta)\Bigg[\left(\frac{\gamma}{\omega+\eta}\right)[(\omega+\eta)+\gamma\mathcal{H}(\vartheta)]+(\omega+\eta)q\Bigg]\\&+\vartheta\mathcal{H}_1(\vartheta)(1-\mathcal{G}^*(\gamma))\{[\mathcal{H}_b^*(\mathcal{H}_1(\vartheta))\mathcal{H}(\vartheta)+\mathcal{H}_v^*(\mathcal{H}_2(z))]-1\}\\&+\gamma(1-\mathcal{H}_b^*(\mathcal{H}_1(\vartheta)))\{\vartheta\mathcal{H}(\vartheta)+[\mathcal{H}_v^*(\mathcal{H}_2(\vartheta))-1]\\&[\mathcal{G}^*(\gamma)+\vartheta[1-\mathcal{G}^*(\gamma)]]\}\Bigg\}\end{aligned}$$

where Π_0 *is denoted by eqn.* (28).

Proof. In both the system and orbit, the PGF of the number of iodobenzene is $(\mathcal{K}(\vartheta))$, $(\mathcal{K}_0(\vartheta))$ is calculated by using $\mathcal{K}(\vartheta)=\Pi_0+\Upsilon_0+\Upsilon(\vartheta)+\vartheta(\Theta_b(\vartheta)+\Delta_v(\vartheta))$ and $\mathcal{K}_0(\vartheta)=\Pi_0+\Upsilon_0+\Upsilon(\vartheta)+\Theta_b(\vartheta)+\Delta_v(\vartheta)$. The eqns. (30) and (31) may be derived directly when the eqns. (25)-(28) are substituted in the earlier results. ■

4 System performance

This section contains the model's estimated average busy duration for various system states, as well as some important system probability and system efficiency measurements.

4.1 Measures of the system's efficiency

Utilizing eqns, (25)-(27), we obtain the findings shown in below, giving $\check{\zeta} \to 1$ using L'Hospital's rule.

(i) Let Υ be the SS Pr(of the server is available during the retrial),

$$\begin{aligned}\Upsilon &= \Upsilon(1) \\ &= \Pi_0\gamma\xi(1-\mathcal{G}^*(\gamma))\left\{\frac{(1-\mathcal{H}_v^*(\omega+\eta))\big(\frac{1}{\omega+\eta}-\mathcal{E}(\mathcal{H}_b)\big)-[\big(\frac{\omega+\eta}{\gamma}q\big)]}{\mathcal{G}^*(\gamma)+\gamma\xi\mathcal{E}(\mathcal{H}_b)}\right\}\end{aligned} \tag{32}$$

(ii) Let Θ_b be the SS (Pr that the server is full),

$$\Theta_b = \Theta_b(1) = \Pi_0\gamma\mathcal{E}(\mathcal{H}_b)\left\{\frac{(\mathcal{H}_v^*(\omega+\eta)-1)\big(\frac{\gamma\xi}{\omega+\eta}+\mathcal{G}^*(\gamma)\big)}{\mathcal{G}^*(\gamma)+\gamma\xi\mathcal{E}(\mathcal{H}_b)}\right\} \tag{33}$$

(iii) Let Δ_v be the SS Pr (the server is on hybrid vacation),

$$\Delta_v = \Delta_v(1) = \frac{\gamma\Pi_0}{\omega+\eta}[1-\mathcal{H}_v^*(\omega+\eta)] \tag{34}$$

4.2 Mean queue length

When the system is in steady state,

(i) With regard to ϑ, (31) and giving $\vartheta = 1$ yields the mean number of iodobenzene in the orbit $(\mathcal{L}_q)$

$$\mathcal{L}_q = \mathcal{K}_0^{'}(1) = \lim_{\vartheta\to 1}\frac{d}{d\vartheta}\mathcal{K}_0(\vartheta) = \Pi_0\left[\frac{\mathcal{N}_q^{'''}(1)\mathcal{D}_q^{''}(1)-\mathcal{D}_q^{'''}(1)\mathcal{N}_q^{''}(1)}{3(\mathcal{D}_q^{''}(1))^2}\right] \tag{35}$$

$$\mathcal{N}_q^{''}(1) = -2\gamma\xi\Bigg\{\mathcal{G}^*(\gamma)+\gamma\xi\mathcal{E}(\mathcal{H}_b)+\frac{\gamma}{(\omega+\eta)}(1-\mathcal{H}_v^*(\omega+\eta))$$
$$\Bigg(\mathcal{G}^*(\gamma)[1-2\xi-(\omega+\eta)\mathcal{E}(H_b)(1-\xi)]$$
$$+\xi[1-(\omega+\eta)E(\mathcal{H}_b)]-\Bigg(\frac{\omega+\eta}{\gamma}\Bigg)q\Bigg)\Bigg\}$$
$$\mathcal{D}_q^{''}(1) = -2\gamma\xi[\mathcal{G}^*(\gamma)+\gamma\xi\mathcal{E}(\mathcal{H}_b)]$$
$$\mathcal{N}_q^{'''}(1) = \frac{-6\gamma^3\xi^2}{(\omega+\eta)^2}\Bigg\{[\mathcal{G}^*(\gamma)+\gamma\xi\mathcal{E}(\mathcal{H}_b)]\Bigg((\omega+\eta)\mathcal{E}(\mathcal{H}_v)-\mathcal{H}_v^*(\omega+\eta)+1\Bigg)\Bigg\}$$
$$+\mathcal{D}_q^{'''}(1)\Bigg[1+\frac{\gamma}{(\omega+\eta)}(1-\mathcal{H}_v^*(\omega+\eta))\Bigg]-3\gamma\xi(1-\mathcal{G}^*(\gamma))$$
$$\Bigg\{2\gamma\xi[(1-\mathcal{H}_v^*(\omega+\eta))\big(\frac{1}{\omega+\eta}-\mathcal{E}(\mathcal{H}_b)\big)]-2\gamma\xi\mathcal{E}(\mathcal{H}_b)$$
$$\Bigg\{\frac{\gamma\xi}{(\omega+\eta)}[(\omega+\eta)\mathcal{E}(\mathcal{H}_v)-\mathcal{H}_v^*(\omega+\eta)+1]\Bigg\}+\mathcal{H}^{''}(1)$$
$$+(\gamma\xi)^2\mathcal{E}(\mathcal{H}_b^2)(1-\mathcal{H}_v^*(\omega+\eta))+(\gamma\xi)^2\mathcal{E}(\mathcal{H}_v^2)\Bigg\}$$
$$+3\gamma\Bigg\{\gamma\xi\mathcal{E}(\mathcal{H}_b)[\mathcal{H}^{''}(1)+2\Bigg\{\frac{\gamma\xi}{(\omega+\eta)}[(\omega+\eta)\mathcal{E}(\mathcal{H}_v)$$
$$-\mathcal{H}_v^*(\omega+\eta)+1]\Bigg\}-2\gamma\xi(1-\mathcal{G}^*(\gamma))\mathcal{E}(\mathcal{H}_v)]-(\gamma\xi)^2\mathcal{E}(\mathcal{H}_b^2)$$
$$[(1-\mathcal{H}_v^*(\omega+\eta))\big(\frac{\gamma\xi}{\omega+\eta}+\mathcal{G}^*(\gamma)\big)]\Bigg\}$$

$$\mathcal{D}_q^{'''}(1) = -3(\gamma\xi)^2\{\mathcal{E}(\mathcal{H}_b^2)+2(1-\mathcal{G}^*(\gamma))\mathcal{E}(\mathcal{H}_b)\}$$

where $\mathcal{H}^{''}(1)=\frac{(\gamma\xi)^2}{(\omega+\eta)^2}\Bigg\{2[(\omega+\eta)\mathcal{E}(\mathcal{H}_v)-\mathcal{H}_v^*(\omega+\eta)+1]-(\omega+\eta)^2\mathcal{E}(\mathcal{H}_v^2)\Bigg\}$

(ii) With regard to ϑ, (30) and providing $\vartheta=1$ yields the mean number of iodobenzene in the system (L_s)

$$\mathcal{L}_s = K_s^{'}(1)=\lim_{\vartheta\to 1}\frac{d}{d\vartheta}\mathcal{K}(\vartheta)=\Pi_0\left[\frac{\mathcal{N}_s^{'''}(1)\mathcal{D}_q^{''}(1)-\mathcal{D}_q^{'''}(1)\mathcal{N}_q^{''}(1)}{3(\mathcal{D}_q^{''}(1))^2}\right] \quad (36)$$

$$\mathcal{N}_s^{'''}(1) = \mathcal{N}_q^{'''}(1)+6\gamma^2\xi\mathcal{E}(\mathcal{H}_b)\Bigg\{(1-\mathcal{H}_v^*(\omega+\eta))(\frac{\gamma\xi}{\omega+\eta}+\mathcal{G}^*(\gamma))\Bigg\}$$

(iii) Using Little's method, we can estimate both the average waiting

time of iodobenzene in the system ($\mathcal{W}_s$) and the average waiting time of iodobenzene in the queue ($\mathcal{W}_q$). $\mathcal{W}_s = \frac{\mathcal{L}_s}{\gamma}$ and $\mathcal{W}_q = \frac{L_q}{\gamma}$, respectively.

4.3 Mean busy period and cycle

Let $\mathcal{A}(\mathcal{T}_y)$ and $\mathcal{A}(\mathcal{T}_\vartheta)$ represent the expected and predicted size of the busy period and cycle. Then, the results make sense when considering the alternate renewal procedure [21], which leads to

$$\begin{aligned}
&\Pi_0 = \frac{A(\mathcal{T}_0)}{\mathcal{A}(\mathcal{T}_y) + \mathcal{A}(\mathcal{T}_0)}; \mathcal{A}(\mathcal{T}_y) = \frac{1}{\gamma}\left(\frac{1}{\Pi_0} - 1\right); \\
&\mathcal{A}(\mathcal{T}_\vartheta) = \frac{1}{\gamma\Pi_0} = \mathcal{A}(\mathcal{T}_0) + \mathcal{A}(\mathcal{T}_y).
\end{aligned} \tag{37}$$

where $\mathcal{T}_0$ amount of time the system was in its empty condition. As the duration between the arrivals of two iodobenzene differs exponentially. We have the equation $\mathcal{A}(\mathcal{T}_0) = (1/\gamma)$. with variable γ. We may recover (28) by applying (37) the previously discovered results,

$$\begin{aligned}
&\mathcal{A}(\mathcal{T}_y) = \frac{1}{\gamma} \\
&\times \left\{ \begin{array}{l} \mathcal{G}^*(\gamma) + \gamma\xi\mathcal{E}(\mathcal{H}_b)\mathcal{H}_v^*(\omega+\eta) + \gamma[1 - \mathcal{H}_v^*(\omega+\eta)] \\ \qquad \left\{ \frac{\mathcal{G}^*(\gamma)+\xi(1-\mathcal{G}^*(\gamma))}{\omega+\eta} - \mathcal{G}^*(\gamma)\mathcal{E}(\mathcal{H}_b)(1-\xi) \right\} \\ \qquad\qquad + q\xi(\omega+\eta)[\mathcal{G}^*(\gamma) - 1] \\ \hline \mathcal{G}^*(\gamma) + \gamma\xi\mathcal{E}(\mathcal{H}_b) \end{array} - 1 \right\}
\end{aligned} \tag{38}$$

$$\begin{aligned}
&\mathcal{A}(\mathcal{T}_\vartheta) = \frac{1}{\gamma} \\
&\times \left\{ \begin{array}{l} \mathcal{G}^*(\gamma) + \gamma\xi\mathcal{E}(\mathcal{H}_b)\mathcal{H}_v^*(\omega+\eta) + \gamma[1 - \mathcal{H}_v^*(\omega+\eta)] \\ \qquad \left\{ \frac{\mathcal{G}^*(\gamma)+\xi(1-\mathcal{G}^*(\gamma))}{\omega+\eta} - \mathcal{G}^*(\gamma)\mathcal{E}(\mathcal{H}_b)(1-\xi) \right\} \\ \qquad\qquad + q\xi(\omega+\eta)[\mathcal{G}^*(\gamma) - 1] \\ \hline \mathcal{G}^*(\gamma) + \gamma\xi\mathcal{E}(\mathcal{H}_b) \end{array} \right\}
\end{aligned} \tag{39}$$

4.4 Special cases

In this section, we examine a few real-world examples of our strategy that are consistent with recent literature.

Case (i):

Let $\omega, \eta = 0$, $\xi = 1$ and $\mathcal{G}^*(\gamma) \to 1$. Our model can be simplified to a $M/G/1$ queue. The results agree with Takagi [20].

$$\mathcal{K}(\vartheta) = \Pi_0 \left\{ \frac{\mathcal{N}e(\vartheta)}{\mathcal{D}e(\vartheta)} \right\} \tag{40}$$

$$\begin{aligned}
\mathcal{N}e(\vartheta) =& (1-\vartheta)\{\vartheta - \mathcal{H}_b^*(\gamma(1-\vartheta))\} + \vartheta(1 - \mathcal{H}_b^*(\gamma(1-\vartheta))) \\
& \{\mathcal{H}_v^*(\gamma(1-\vartheta)) - 1\} \\
\mathcal{D}e(\vartheta) =& (1-\vartheta)\{\vartheta - \mathcal{H}_b^*(\gamma(1-\vartheta))\}
\end{aligned}$$

Case (ii):

Let $\omega, \eta = 0$ and $\xi = 1$. Our model can be simplified to an $M/G/1$ RQ. Then the results agree with Gao and Wang [21].

$$\mathcal{K}(\vartheta) = \Pi_0 \left\{ \frac{\mathcal{N}e(\vartheta)}{\mathcal{D}e(\vartheta)} \right\} \tag{41}$$

$$\begin{aligned}
\mathcal{N}e(\vartheta) =& \gamma(1-\vartheta)\{\vartheta - [\mathcal{G}^*(\gamma) + \vartheta(1 - \mathcal{G}^*(\gamma))]\mathcal{H}_b^*(\gamma(1-\vartheta))\} \\
& + \vartheta\gamma(1-\vartheta)[1 - \mathcal{G}^*(\gamma)](\mathcal{H}_v^*(\gamma(1-\vartheta)) - 1) \\
& + \gamma\vartheta[1 - \mathcal{H}_b^*(\gamma(1-\vartheta))]\{\mathcal{H}_v^*(\gamma(1-\vartheta) - 1) \\
& [\mathcal{G}^*(\gamma) + \vartheta(1 - \mathcal{G}^*(\gamma))]\} \\
\mathcal{D}e(\vartheta) =& \gamma(1-\vartheta)\{\vartheta - [\mathcal{G}^*(\gamma) + \vartheta(1 - \mathcal{G}^*(\gamma))]\mathcal{H}_b^*(\gamma(1-\vartheta))\}
\end{aligned}$$

Case (iii):

Let $\eta = 0$ and $\mathcal{G}^*(\gamma) \to 1$. Our model simplified to an $M/G/1$ queue with WV. Then the results agree with Zhang and Hou [22].

$$\mathcal{K}(\vartheta) = \Pi_0 \left\{ \frac{\mathcal{N}e(\vartheta)}{\mathcal{D}e(\vartheta)} \right\} \tag{42}$$

$$\mathcal{N}e(\vartheta) = \left\{\omega(1+q)+\gamma\vartheta\left(\frac{1-H_v^*(\omega+\gamma\xi(1-\vartheta))}{\omega+\gamma\xi(1-\vartheta)}\right)\right\}$$
$$\mathcal{H}_1(\vartheta)[\vartheta-\mathcal{H}_b^*(\mathcal{H}_1(\vartheta))]+\gamma\vartheta[1-\mathcal{H}_b^*(\gamma(1-\vartheta))]$$
$$\left\{\vartheta\omega\left(\frac{1-H_v^*(\omega+\gamma\xi(1-\vartheta))}{\omega+\gamma\xi(1-\vartheta)}\right)+[\mathcal{H}_v^*(\omega+\gamma\xi(1-\vartheta))-1]\right\}$$
$$\mathcal{D}e(\vartheta) = \mathcal{H}_1(\vartheta)\{\vartheta-\mathcal{H}_b^*(\mathcal{H}_1(\vartheta))\}$$

where, $\Pi_0 = \dfrac{\gamma\xi\mathcal{E}(\mathcal{H}_b)}{\gamma\xi\mathcal{E}(\mathcal{H}_b)\mathcal{H}_v^*(\omega)-\gamma(1-\mathcal{H}_v^*(\omega))\left[\frac{1}{\omega}-\mathcal{E}(\mathcal{H}_b)(1-\xi)\right]}$

5 Numerical results

The various effects on system performance measurements are demonstrated using MATLAB in this section. We examine exponentially distributed retrial times, service times, and slower service times. A random selection is made from among the numerical measurements that are suitable for the stability criteria.

Table 1 clearly displays that retrial rate $G^*(\gamma)$ escalates, $\mathcal{L}_q$, $\mathcal{L}_s$, Δ_v are decreases. Table 2 clearly displays that the hybrid vacation rate ζ_v increases, $\mathcal{L}_q$, $\mathcal{L}_s$, are decreases and Π_0 increases. Table 3 displays that lower service rate ω escalates, $\mathcal{L}_q$, $\mathcal{L}_s$, Δ_v and Π_0 decreases.

Table 1. Π_0 and $\mathcal{L}_q$ for various retrial rate $\mathcal{G}^*(\gamma)$ for the parameter values of $\gamma = 0.6$, $\xi = 0.5$, $q = 1$, $\eta = 0.5$, $\omega = 0.6$, $\zeta_b = 0.8$ and $\zeta_v = 0.9$

Retrial rate $G^*(\gamma)$	Π_0	$\mathcal{L}_q$	$\mathcal{L}_s$	$\mathcal{W}_q$	Υ	Δ_v
3.1	0.8044	4.6846	5.3800	7.8076	0.1675	0.0689
3.2	0.8020	4.2440	4.8633	7.0734	0.1698	0.0687
3.3	0.7998	3.8867	4.4448	6.4779	0.1721	0.0686
3.4	0.7977	3.5917	4.0997	5.9861	0.1742	0.0684
3.5	0.7957	3.3446	3.8110	5.7425	0.1761	0.0682
3.6	0.7939	3.1349	3.5663	5.2248	0.1780	0.0681
3.7	0.7922	2.9549	3.3566	4.9249	0.1798	0.0679

With the impact of the parameters q γ, ω, ξ, ζ_b, ζ_v, The system per-

Table 2. Π_0 and $\mathcal{L}_q$ for various hybrid vacation rate (ζ_v) for the parameter values of $\gamma = 1.5$, $\xi = 0.02$, $q = 1$, $\eta = 0.02$, $\omega = 0.1$, $\zeta_b = 0.9$ and $\mathcal{G}^*(\gamma) = 0.5$

Hybrid vacation rate (ζ_v)	Π_0	$\mathcal{L}_q$	$\mathcal{L}_s$	$\mathcal{W}_q$	Υ	Δ_v
0.5	0.4328	6.8324	20.3312	4.5550	0.0104	2.7048
0.55	0.4588	6.5779	19.4584	4.3853	0.0098	2.5809
0.6	0.4882	6.2806	18.4636	4.1871	0.0091	2.4411
0.65	0.5217	5.9344	17.3243	3.9562	0.0085	2.2822
0.7	0.5600	5.5305	16.0109	3.6870	0.0077	2.1000
0.75	0.6044	5.0568	14.4833	3.3712	0.0067	1.8888
0.8	0.6565	4.4965	12.6875	2.9977	0.0056	1.6412

Table 3. Π_0 and $\mathcal{L}_q$ for various lower service rate (ω) for the parameter values of $\gamma = 2$, $\xi = 0.9$, $q = 1$, $\eta = 5$, $\mathcal{G}^*(\gamma) = 5$, $\zeta_b = 0.9$ and $\zeta_v = 6$

Lower service rate (ω)	Π_0	$\mathcal{L}_q$	$\mathcal{L}_s$	$\mathcal{W}_q$	Υ	Δ_v
1	0.4418	0.0163	0.0189	0.0081	0.7213	0.0147
2	0.4019	0.0149	0.0173	0.0075	0.7474	0.0115
3	0.3678	0.0137	0.0159	0.0069	0.7689	0.0092
4	0.3394	0.0127	0.0147	0.0064	0.7871	0.0075
5	0.3151	0.0118	0.0137	0.0059	0.8026	0.0063
6	0.2940	0.0110	0.0128	0.0055	0.8160	0.0053
7	0.2755	0.0104	0.0120	0.0052	0.8276	0.0046

formance metrics are depicted in a two-dimensional plot, which is shown in Fig. 3. In Fig. 3(a), displays the escalation of the retrial rate $G^*(\gamma)$, and ($\mathcal{L}_q$), ($\mathcal{L}_s$), (Π_0) are decreases. In Fig. 3(b), we found that ($\mathcal{L}_s$), (Υ), and Δ_v decreases while increase the hybrid vacation rate ζ_v.

The three-dimensional graph representing the system performance metrics is shown in Fig. 4. In Fig. 4(a), the surface displays the elevation the retrial rate $G^*(\gamma)$ and (Υ), (Π_0) are diminishes. In Fig. 4(b), we found that $\mathcal{L}_s$ diminishes while increasing the hybrid vacation rate (ζ_v), (Π_0). In Fig. 4(c), we found that (Π_0) and (Δ_v) diminishes while increasing the lower service rate ω.

The numerical findings presented earlier can be utilized to ascertain

the influence that attributes have on the evaluation criteria of the system, and we can be certain that the results are accurate reflections of the circumstances in concern.

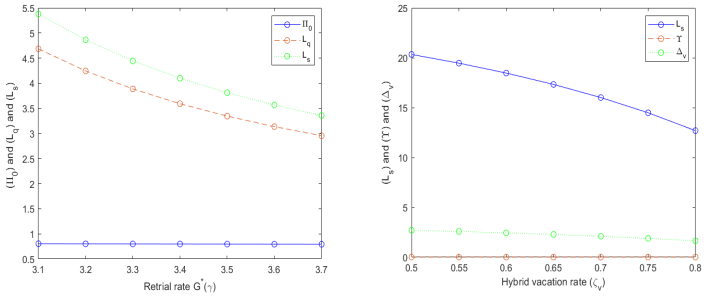

(a) Π_0, $\mathcal{L}_q$, $\mathcal{L}_s$ vs retrial rate $G^*(\gamma)$ (b) L_s, Υ, Δ_v vs hybrid vacation rate ζ_v

Figure 3. 2D visualization of $\mathcal{G}^*(\gamma)$ and ζ_v

6 Computing of ANFIS

Adaptive neuro-fuzzy inference systems, or ANFIS, are a type of artificial neural network that heavily borrows from evolutionary network fuzzy inference systems. Early in the 1990s, Jang [23] developed the ANFIS methodology. Because it incorporates both neural networks and fuzzy logic concepts, it may harness the benefits of both in a single framework. The ANFIS is often regarded as a trustworthy estimator of anything. The soft computing approach of ANFIS is a great tool for delivering significant outcomes in actual, daily situations.

Furthermore, the structure of the adaptive network is comprised of nodes and arrow linkages. The outputs of the nodes and the method by which their variables can be changed to reduce a specified error measure are both specified in the node variables. To get the intended mapping between input and output, the parameters are changed using gradient-based techniques and training data. Considering that people understand a type of logic and often store input-output information as combinations, ANFIS

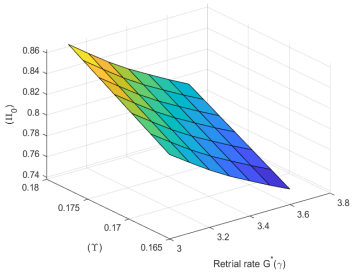

(a) Υ, Π_0 vs retrial rate $G^*(\gamma)$

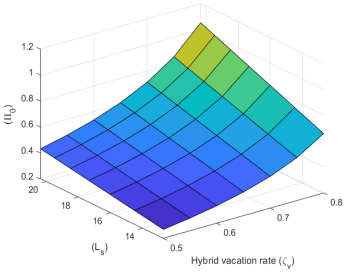

(b) Π_0, $\mathcal{L}_s$ vs hybrid vacation rate ζ_v

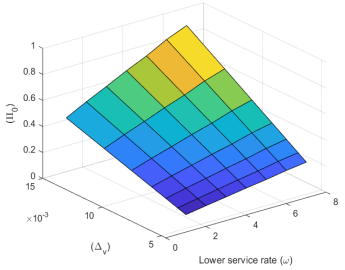

(c) Π_0, Δ_v vs lower service rate ω

Figure 4. 3D visualization of $\mathcal{G}^*(\gamma)$, ζ_v, and ω

may be utilized to construct an input-output mapping. The direct search approach is cumbersome to utilize due to the time restrictions produced by the repetitive repeating of the procedure to discover the best attainable response. ANFIS has the capacity to execute flexible data processing. The general configuration of the ANFIS is seen in Fig. 5. When exact solutions for particular performance indices are difficult to get the accurate approximations, one can use of ANFIS. In this part, we compare the neuro-fuzzy findings of SVT and PGF analyses utilizing ANFIS technology.

Some elements are identified as linguistic words and used as inputs to connect a fuzzy method to ANFIS technique. Assuming a Gaussian membership function for each of these input variables which is depicted in its corresponding form in Fig. 6. Table 4 shows the membership count function, as well as the relevant parameter values and languages.

We use MATLAB programme for analytically determining ANFIS val-

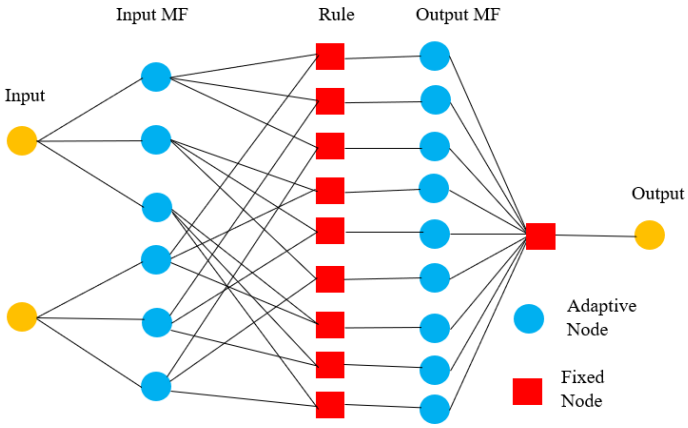

Figure 5. Pictorial representation of ANFIS

Table 4. Terms of the membership functions determined on the input parameters' language

Input values	Count of membership-related functions	Linguistic types
$G^*(\gamma)$, ζ_v, ω	3	Low, Medium, High

ues. For each of the following values of L_q, L_s, and Δ_v, we compute the ranges of $G^*(\gamma)$, ζ_v, and ω from 0 to 8. The results of the ANFIS are shown by the discrete lines in Fig. 7, whereas the continuous lines represent the exponential function. Fig. 8 illustrates the usage of ANFIS to depict the $G^*(\gamma)$, ζ_v, and ω in 3-D visualization. Ultimately, we found that there were similarities between the ANFIS and exponential function outcomes.

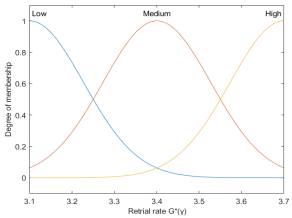

(a) Membership Function of $G^*(\gamma)$

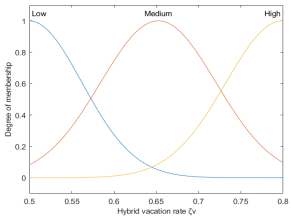

(b) Membership Function of ζ_v

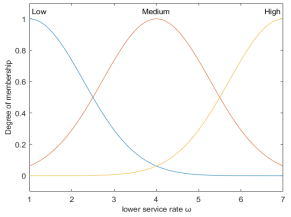

(c) Membership Function of ω

Figure 6. Membership Function

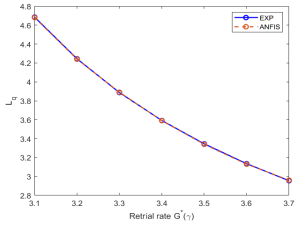

(a) $\mathcal{L}_q$ vs $G^*(\gamma)$,

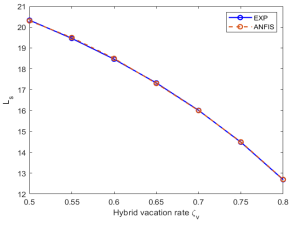

(b) $\mathcal{L}_S$ vs ζ_v

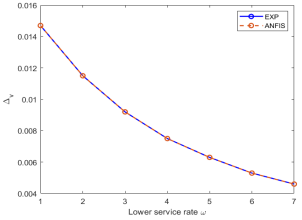

(c) Δ_v versus ω

Figure 7. Relation between exponential function and ANFIS

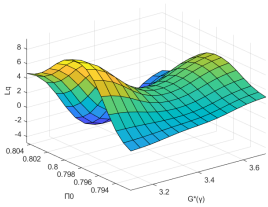

(a) L_q and Π_0 vs $G^*(\gamma)$

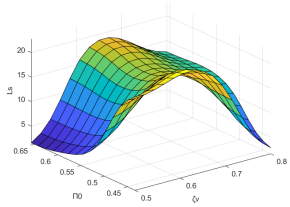

(b) L_s and Π_0 vs ζ_v

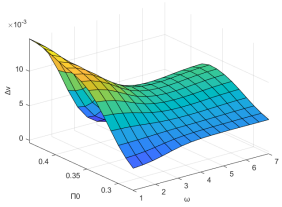

(c) Δ_v and Π_0 versus ω

Figure 8. ANFIS-based 3D visualization of $G^*(\gamma)$, ζ_v and ω

7 Conclusion

In summary, we have developed the first chemical retrial queue model for the Ullmann reaction when combined with a hybrid vacation policy. We observed that stabilization of the system is possible if all necessary and sufficient conditions are satisfied. While using the PGF method and the supplementary variable technique, we can determine the PGF of the number of systems and their orbits when the systems are free, busy, or on hybrid vacation. Ultimately, a variety of numerical results are presented and used to analyze the effect of system characteristics. Moreover, the performance indices are computed using the numerical method of the soft computing approach ANFIS in order to confirm the validity of the existing model for real-time systems. We anticipate that the suggested model, which makes use of fuzzy parameters using an ANFIS approach, will be especially helpful for chemists conducting high-throughput reaction discovery as well as improving Ullmann's reaction performance. It

also finds application among system engineers who are developing the accurate queueing models.

***Acknowledgment*:** The authors would like to thank the anonymous reviewers for their valuable comments and suggestions. Further, the authors would like to express their heartfelt gratitude to Mr. R. Sreedharan and Mr. S. Suresh, Department of Chemistry, Vellore Institute of Technology, Vellore, India, for their comprehensive input in shaping the quality of the paper.

References

[1] W. Bohm, K. Hormik, On two-periodic random walks with boundaries, *Stoch. Models* **26** (2010) 165–194.

[2] W. H. Stockmeyer, W. Gobush, R. Norvich, Local-jump models for chain dynamics, *Pure Appl. Chem.* **26** (1971) 537–543.

[3] B. W. Conolly, P. R. Parthasarathy, S. Dharmaraja, A chemical queue, *Math. Sci.* **22** (1997) 83–91.

[4] A. M. K. Tarabia, A. H. El-Baz, Transient solution of a random walk with chemical rule, *Phys. A Stat. Mech.* **382** (2007) 430–438.

[5] A. M. K. Tarabia, Analysis of random Walks with an absorbing Barrier and chemical rule, *J. Comput. Appl. Math.* **225** (2009) 612–620.

[6] S. Tsitkov, T. Pesenti, H. Palacci, J. Blanchet, H. Hess, A queueing theory-based perspective of the kinetics of "channeled" enzyme cascade reactions, *ACS Catal.* **8** (2018) 10721–10731.

[7] G. Alshreef, A. Tarabia, Transient analysis of chemical queue with catastrophes and server repair, *Inf. Sci. Lett.* **12** (2023) 541–545.

[8] E. Sperotto, G. P. M. van Klink, G. van Koten, J. G. de Vries, The mechanism of the modified Ullmann reaction, *Dalton Trans.* **43** (2010) 10338–10351.

[9] J. P. Finet, S. C. Fedorov, G. Boyer, Recent advances in Ullmann reaction: copper (II) diacetate C at alysed N-, O-and S-arylation involving polycoordinate hetero atomic derivatives, *Curr. Org. Chem.* **6** (2002) 597–626.

[10] G. I. Falin, J. G. C. Templeton, *Retrial Queues*, Chapman and Hall, London, 1997.

[11] J. R. Artalejo, Accessible bibliography on retrial queues, *Math. Comput. Model.* **30** (1999) 1–6.

[12] D. Arivudainambi, M. Godhandaraman, P. Rajadurai, Performance analysis of a single server retrial queue with working vacation, *Opsearch.* **33** (2013) 55–81.

[13] V. M. Chandrasekaran, K. Indhira, M. C. Saravanarajan, P. Rajadurai, A survey on working vacation queueing models, *Int. J. Pure. Appl. Math.* **106** (2016) 33–41.

[14] P. Rajadurai, Sensitivity analysis of an $M/G/1$ retrial queueing system with disaster under working vacations and working breakdowns, *RAIRO Oper. Res.* **52** (2018) 35–54.

[15] C. Revathi, L. Francis Raj, Search of Arrivals of an $M/G/1$ retrial Queueing system with delayed repair and optional re-service using modified Bernoulli vacation, *J. Comput. Math.* **6** (2022) 200–209.

[16] S. Maragathasundari, B. Balamurugan, Analysis of an $M^{[X]}/G/1$ feedback queue with two stages of repair times, general delay time, *Int. J. Appl. Eng.* **10** (2015) 25165–25174.

[17] M. M. N. GnanaSekar, I. Kandaiyan, Analysis of an $M/G/1$ retrial queue with delayed repair and feedback under working vacation policy with impatient customers, *Symmetry* **14** (2022) #2024.

[18] A.G. Pakes, Some conditions for Ergodicity and recurrence of Markov chains, *Oper. Res.* **17** (1969) 1058–1061.

[19] S. T. Humblet, Average drifts and the non-Ergodicity of Markov chains, *Oper. Res.* **31** (1983) 783–789.

[20] H. Takagi, *Vacation and Priority Systems, Part I. Queueing Analysis: A Foundation of Performance Evaluation*, North-Holland, Amsterdam, New York, (1991).

[21] S. Gao, J. Wang, W. Li, An $M/G/1$ retrial queue with general retrial times, working vacations and vacation interruption, *Asia Pac. J. Oper. Res.* **31** (2014) 6–31.

[22] M. Zhang, Z. Hou, $M/G/1$ queue with single working vacation, *J. Appl. Math. Comput.* **39** (2012) 221–234.

[23] J. S. R. Jang, ANFIS: adaptive-network-based fuzzy inference system, *IEEE Trans. Syst. Man Cybern.* **23** (1993) 665–685.